Available online at www.sciencedirect.com
SCIENCE DIRECT®
Journal of Solid State Chemistry 177 (2004) 431–438
JOURNAL OF SOLID STATE CHEMISTRY
http://elsevier.com/locate/jssc

New quaternary carbon and nitrogen stabilized polyborides: $RE B_{15.5}CN$ (*RE*: Sc, Y, Ho, Er, Tm, Lu), crystal structure and compound formation

A. Leithe-Jasper,[1] T. Tanaka,* L. Bourgeois,[2] T. Mori, and Y. Michiue

Advanced Materials Laboratory, National Institute for Materials Science, Namiki 1-1, Tsukuba, Ibaraki 305-0044, Japan

Received 14 November 2002; accepted 18 February 2003

Abstract

A new family of quaternary carbon and nitrogen containing Rare Earth (*RE*: Sc, Y, Ho, Er, Tm and Lu) borides: $RE B_{15.5}CN$, has been synthesized and structurally characterized by powder X-ray diffraction data. They are all isotypic with $Sc_{1-x}B_{15.5}CN$ whose structure was solved based on single-crystal X-ray data and HRTEM investigations. The structure refinement converged at a $R(F^2)$ value of 0.044 for 364 reflections. The new structure type of $Sc_{1-x}B_{15.5}CN$ is composed of a three-dimensional network based on interconnected slabs of boron $(B_{12})^{ico}$ icosahedra and $(B_6)^{oct}$ octahedra. A linear [CBC] chain and nitrogen tightly bridges icosahedra. Sc partially occupies voids in the sheets of boron octahedra. It crystallizes with the trigonal space group P^3m1, with $Z = 2$. Lattice parameters (nm) are as follows: for *RE*: Sc, $a, b = 0.5568(4)$, $c = 1.0756(2)$; Y, $a, b = 0.55919(6)$, $c = 1.0873(2)$; Ho, $a, b = 0.55883(7)$, $c = 1.0878(6)$; Er, $a, b = 0.55889(5)$, $c = 1.0880(6)$; Tm, $a, b = 0.5580(1)$, $c = 1.0850(6)$; Lu, $a, b = 0.55771(9)$, $c = 1.0839(4)$. Magnetic characterization of $ErB_{17}C_{1.3}N_{0.6}$ has been performed.

Keywords: Rare earth borides; Crystal structure; Scandium borocarbide; Boron clusters

1. Introduction

The crystal structures of boron rich compounds are governed by a three-dimensional arrangement of clusters formed by boron atoms, namely $(B_6)^{oct}$ octahedra and $(B_{12})^{ico}$ icosahedra as well as other polyhedra. All of these compounds exhibit significant hardness and a refractory nature which can be correlated with a strong bonding in the networks of the linked boron polyhedra [1].

Recently, we have reported the synthesis of a series of compounds in Rare-Earth (*RE*) boron carbon and/or nitrogen systems, in which $(B_{12})^{ico}$ and $(B_6)^{oct}$ build homologous phases with crystal structures generated by different stacking sequences of structural motifs found in "B_4C" [2–4].

Here we want to give a detailed discussion of the synthesis and crystal structure of the family of $RE B_{15.5}CN$ (*RE*: Sc, Y, Ho, Er, Tm and Lu) compounds which represents the starting member of this remarkable series.

2. Experimental procedures

2.1. Crystal growth of $Sc_{1-x}B_{15.5}CN$

In a typical experiment about 1 g of a "$ScB_{17}C$" master alloy was powdered and mixed with Sn powder followed by cold isostatic pressing into a cylindrical bar. This rod was placed in a crucible made from sintered BN which was inserted into a graphite susceptor with a cap. Under a flow of Ar gas this setup was quickly (within 1 h) inductively heated up to 1600°C, kept there for 6–8 h and cooled down to room temperature (100°C/h). The tin matrix was dissolved by leaching in warm concentrated HCl. Silver gray agglomerates of intergrown hexagonal plates with a metallic luster with

*Corresponding author. Fax: 81-298-52-7449.
E-mail address: tanaka.takaho@nims.go.jp (T. Tanaka).
[1] Present address: MPI-CPfS, Dresden, Nöthnitzerstraße 40, D-01187, Germany.
[2] Present address: School of Physics and Materials Engineering, Monash University, P.O. Box 69M, Victoria 3800, Australia.

0022-4596/$ - see front matter © 2003 Elsevier Inc. All rights reserved.
doi:10.1016/j.jssc.2003.02.003

the size of up to $1 \times 0.5 \times 0.5\,mm^3$ were isolated. Crystals can be also grown in a Si flux under similar experimental conditions.

2.2. Bulk synthesis of $REB_{15.5}CN$ phases

Starting materials for the sample production were powders of REB_m (m:12–16) (RE: Rare Earth metal) which were synthesized by boro thermal reduction (in a BN crucible inserted in an inductively heated carbon free TiB_2/BN composite susceptor under dynamic vacuum) according to the following reaction:

$$RE_2O_3 + (2m+3)B \rightarrow 2REB_m + 3BO\uparrow$$

at temperatures up to 1700°C. (Sc_2O_3 powder: 3N, Crystal Systems Inc. Japan; RE_2O_3 powders: 3N, Rare Metallics Co., Japan; amorphous boron: 3N, SB-Boron Inc. USA and graphite powder: 3N, Koujundo Kagaku Co., Japan.) Then the desired amounts of carbon and hexagonal BN (4N, Showa Denko Co., Japan) were added to the powdered sample and fired again at 1600°C in a graphite susceptor under a flow of Ar-gas. Typical reaction paths could be read as

$$REB_{14.5} + BN + C \rightarrow REB_{15.5}CN,$$

$$REB_{12} + 2.5B + BN + C \rightarrow REB_{15.5}CN.$$

Quotation marks mean that in nearly all cases the product was not single phase but contained additional binary rare earth borides (REB_6 and/or REB_{12}) or in case of Sc the compound $ScB_{17}C_{0.25}$ [5]. The best yields with respect to phase purity could be achieved in the case of (Ho,Er)$B_{15.5}CN$ (qualitatively about 95% yield, judged from powder X-ray diffraction). In case of a REB_6 contamination treatment in warm diluted HNO_3/H_2O (1:2) could dissolve the hexaboride phases without attacking the $REB_{15.5}CN$ phases. Because of the much higher chemical inertness of the rare earth dodecaborides, REB_{12} impurities could not be removed from the samples by acid leaching.

The addition of carbon as graphite powder is an essential step to produce $REB_{15.5}CN$ phases in significant amounts. If the reaction starts from prereacted "$REB_{14.5}C$" and BN is added, compound formation is only sluggishly achieved. Already at 1600°C free carbon seems to catalyze the decomposition of hex-BN which obviously facilitates the formation of the quaternary compounds. Under dynamic vacuum this kind of synthesis of $REB_{15.5}CN$ can be also performed though reaction yields are not satisfying.

Another possibility to synthesize the $REB_{15.5}CN$ (RE: Sc, Y, Ho, Er, Tm, Lu) compounds represents the introduction of nitrogen via the gas phase. Here we started with samples of "$REB_{15.5}C$" composition. Though reaction under pure nitrogen gas at 1600°C leads to complete decomposition of the starting materials, a "small" partial pressure of nitrogen produced inside the reaction unit (in these experiments only via "reaction" of the BN container with the hot graphite susceptor) is sufficient for quaternary compound formation within a few hours.

2.3. Chemical characterizations

The chemical composition of several crystals grown in a Si and Sn-flux were checked by EPMA. Standards in the form of FZ-grown crystals of ScB_{12} [17], $B_{4.3}C$ [18] and hex-BN (their compositions were established by wet chemical analysis) were used to deduce the stoichiometry. Special attention was paid to possible Si or Sn inclusions. The compositions of the crystals were found to lay in the range of $ScB_{16.3}C_{1.39}N_{1.13}$ (for the crystals grown in the Sn flux) and $ScB_{17}C_{1.58}N_{0.88}$ (for the Si flux experiment). No Sn or Si was detected in the crystals.

For bulk "$ErB_{15.5}CN$" (prior treated with diluted HNO_3) a complete wet chemical analysis was performed. After the powder was dissolved in a HNO_3/HCl (1:1) solution keeping it at 150°C for 16 h, the erbium and boron contents were determined by chelate titration and inductively coupled plasma atomic emission spectroscopy, respectively. The carbon content was determined by a volumetric combustion method using a carbon determinator (WR-12, Leco-Co.). Nitrogen content was measured with a standard inert gas fusion method (TC-436AR, Leco-Co.). A composition of $ErB_{17}C_{1.3}N_{0.6}$ was deduced.

Oxygen impurities were analyzed by a standard inert gas fusion method (TC-136, Leco Co.) and were found to represent 0.07 wt%.

2.4. X-ray diffraction and crystal structure

Phase identification was carried out using a standard X-ray powder diffractometer (R-2000, Rigaku Co.) with Cu$K\alpha$ radiation. The $K\alpha 1$ peak intensities were determined after rejecting $K\alpha 2$ peaks, using RINT software (Rigaku Co).

For several platelet $Sc_{1-x}B_{15.5}CN$ crystal specimen symmetry was checked on a Weissenberg camera (Ni-filtered Cu$K\alpha$-radiation). Equiinclination Weissenberg photographs of several layer-lines were recorded showing a reciprocal space of trigonal symmetry without any special extinctions and no indications of superstructure formation. Single-crystal data collections of a crystal grown in a Si-flux were done on a Rigaku AFC7R rotating anode 4 circle diffractometer (data collection at 60 kV and 200 mA, Mo$K\alpha$) and for a specimen grown from a Sn-flux (results presented here) on a Rigaku AFC7-CCD (data collection at 50 kV and 40 mA, Mo$K\alpha$). The intensity data were corrected for Lorentz and polarization effects. Absorption corrections were empirical based on ψ-scans (3). Details of the

Table 1
Crystallographic and data collection parameters of "$Sc_{1-x}B_{15.5}CN$"

Crystal system	Trigonal
Space group	P^3m1 (No. 164)
a, b (nm)	0.5568(2)[a]
c (nm)	1.0756(2)[a]
Volume (nm^3)	0.2888(2)
Z	2
F_w	226.12
D_x (g/cm^3)	2.842
Applied radiation, λ (nm)	Monochromator Mo$K\alpha$ 0.71073 nm
Linear absorption coefficient μ (mm^{-1})	1.18
Crystal dimensions (mm)	$0.035 \times 0.035 \times 0.0075$
Absorption correction	Empirical (ψ-scans)
Data corrections	Lorentz, polarization
Reflections measured	$0 \leqslant h \leqslant 7$ $-7 \leqslant k \leqslant 6$ $-15 \leqslant l \leqslant 15$
$2\theta_{max}$ (deg)	59.95
Unique reflections	364
Structure refinement program	SHELX97 (based on F_o^2)
Number of variables	41
R_1[b] [$F_o > 4\sigma(F_o)$] (for 314 F_o)	0.044
R_1 [all F_o] (for 364 F_o)	0.054
wR_2 (F^2)[b]	0.115

[a] The lattice constants were determined on the four circle diffractometer.

[b] $R_1 = \sum||F_o| - |F_c||/\sum|F_o|$; w$R_2 = [\sum|w(F_o^2 - F_c^2)^2|/\sum|w(F_o^2)^2|]^{1/2}$, $w = [\sigma^2(F_o^2) + (xP)^2 + yP]^{-1}$, where $P = (\mathrm{Max}(F_o^2, 0) + 2F_c^2)/3$.

crystallographic data and data collection parameters are given in Table 1.

Crystal chemical considerations together with the program SIR92 [6] were used for structure solution and the program SHELXL-97 [7] was used for refinement. In the course of this investigation the graphic program ATOMS [8] was used for visualization and drawing of the structures.

The isostructural nature of all $RE B_{15.5}CN$ phases was deduced from their similar X-ray powder diffraction patterns, complete indexing based on the trigonal unit cell and good match of observed and calculated intensities based on the atomic positions derived for the Sc containing compound.

2.5. Transmission electron microscopy and electron diffraction

High-resolution transmission electron microscopy (HRTEM) and electron diffraction were carried out on a field-emission JEM-3000F (JEOL) instrument operated at 300 kV. HRTEM image simulations by the multi-slice method were performed using the MAC Tempas simulation package with the appropriate electron optical parameters for our microscope. The simulated images presented herein were chosen near the Scherzer defocus of −59 nm, and for crystal thickness resulting in the best match with the experimental image.

2.6. Magnetic characterization

Magnetic susceptibility was measured by using a Quantum Design superconducting quantum interference device (SQUID) magnetometer from 300 K down to 1.8 K under a magnetic field of 50 G.

3. Results and discussion

3.1. Compound formation

In one of our early attempts to grow crystals of $ScB_{17}C_{0.25}$ from a Si metal flux in a BN-crucible [5] a few hexagonal platelets were found as a side product. A single-crystal study led to a crystal structure which was not observed before. From our previous establishment of the Sc–B–C ternary [9] all ternary boron rich phases were known thus giving strong indication of the discovery of a quaternary phase most probably stabilized by nitrogen. Additionally the Rare Earth–B–N phase diagrams recently compiled [10] gave no indication of the formation of boron rich nitrogen containing compounds. The puzzling question in these crystal growth experiments is now the origin and reaction mechanism of the nitrogen incorporation into the compound. As a possible scenario we could envision a decomposition of BN which is in contact with the hot carbon susceptor (see experimental section) catalyzed by traces of oxygen. This assumption is backed by the absence of $Sc_{1-x}B_{15.5}CN$ formation in metal fluxes in the same experimental setup under dynamic vacuum. So a supposedly very small partial pressure of N_2 in the system is sufficient for the compound formation in liquid tin and silicon. Our successful synthesis of bulk material of $RE B_{15.5}CN$ (*RE*: Sc, Y, Ho, Er, Tm, Lu) can be understood as a constructive proof supporting the necessity of nitrogen for compound formation (Table 4). We were not able to synthesize isotypic phases with Rare Earth metal atoms larger than Ho. Synthesis of a Yb containing compound also failed under experimental conditions used in this work.

3.2. Crystal structure description

The crystal structure of $RE B_{15.5}CN$ shows structural features commonly observed in boron rich solids. The three-dimensional boron framework is composed of interconnected boron $(B_6)^{oct}$ octahedra and $(B_{12})^{ico}$ icosahedra. But this particular combination of both of the two well known boron clusters within the rather small unit cell represents an unique arrangement in a diversity of structures usually encountered in solid state chemistry of materials rich in boron. Here we want to point out the striking similarities with the crystal structure of rhombohedral boron carbide "B_4C". In

the hexagonal setting the crystal structure of "B_4C" can be basically understood as a stacking of layers of $(B_{12})^{ico}$ perpendicular to the *c*-axis and [CBC] chains parallel to the *c*-axis linking together with inter-icosahedral bonds the icosahedra in neighboring layers (see Fig. 1b) [11,12]. If now icosahedral layers are replaced in a regular manner by sheets formed by $(B_6)^{oct}$ with interstitial *RE*-atoms, closely related crystal structures of homologous character are generated. It turns out that replacement of every third layer in "B_4C" (see Fig. 1a) already leads to the periodic stacking observed in $Sc_{1-x}B_{15.5}CN$ (which can be understood as $Sc_2(B_6)^{oct}(B_{12})_2^{ico}[CBC]N_2$) which therefore contains two icosahedral sheets between two octahedral slabs. The number of icosahedral layers can increase to three and four in recently synthesized homologous phases $REB_{22}C_3$ and $REB_{28.5}C_4$ [3]. In $Sc_{1-x}B_{15.5}CN$ icosahedra are linked by [CBC] chains, boron octahedra, inter-icosahedral bonds and nitrogen atoms (see Figs. 2a and 3a). Atoms B1–B4 form the $(B_{12})^{ico}$ centered at $(\frac{1}{2},\frac{2}{3},0.8107)$. The interatomic distances $(0.1783 \leqslant d_{BB} \leqslant 0.1828\,nm)$ within the icosahedra are listed in Table 3 with a mean value of 0.1803 nm. The angles within the triangular faces range between 58.85° and 61.45°. Thus no severe distortion of this polyhedron is observed. Of these 12 icosahedral boron atoms 3 B2 atoms form direct inter-icosahedral bonds with $d_{B2B2=}0.1729\,nm$, 3 B1 form bonds with nitrogen ($d_{B1N} = 0.1547\,nm$), 3 B3 atoms are connected with the B5 atoms (forming the octahedra) and 3 B4 are bonded to C with a $d_{B4C}= 0.1587\,nm$. For the linear [CBC] chain we find a bond length of $d_{B6C} = 0.1439\,nm$ (see Fig. 3a).

In rhombohedral "B_4C" we observe interatomic distances within the linear [CBC] chain and between the $(B_{12})^{ico}$ and the chain of 0.1432 and 0.1605 nm, respectively [11,12]. The B4–C bonds observed in $Sc_{1-x}B_{15.5}CN$ deviate from the ideal [13] bonding direction of the normal to the pentagonal pyramid (the "coordination polyhedron" for B4 in the icosahedron is a pentagonal pyramid consisting of 5 next neighboring 2B1, 2B2 and 1B3 atoms and one bonding orbital perpendicular to the pentagonal plane [13] by only 0.38°. In case of "B_4C" a deviation of 0.21° is observed. The inter-icosahedral B2–B2 ($d_{B2B2} = 0.1729\,nm$) bonds however show a deviation of 3.34° compared with 4.8° in "B_4C" ($d_{BB} = 0.1717\,nm$). Those bonds are significantly shorter than the intra-icosahedral bonds (mean

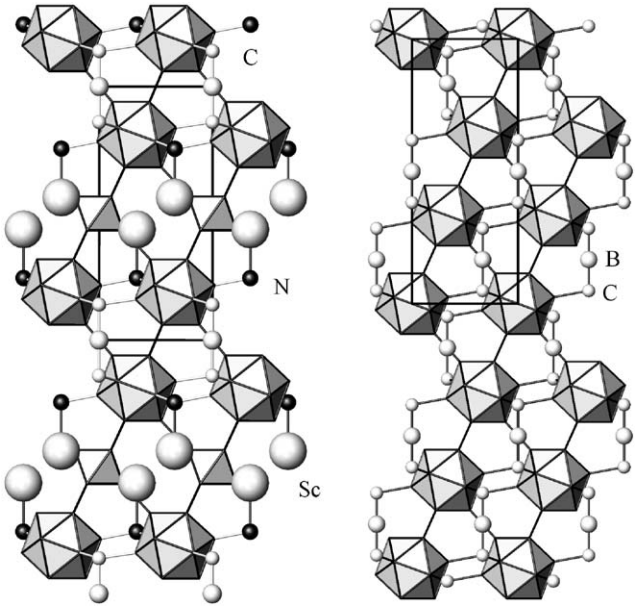

Fig. 1. Comparison of the structures of $Sc_{1-x}B_{15.5}CN$ and "B_4C". Projection along the hexagonal *b*-axis. The polyhedra are boron $(B_6)^{oct}$ octahedra and boron $(B_{12})^{ico}$ icosahedra. (a) $Sc_{1-x}B_{15.5}CN$ and (b) "B_4C".

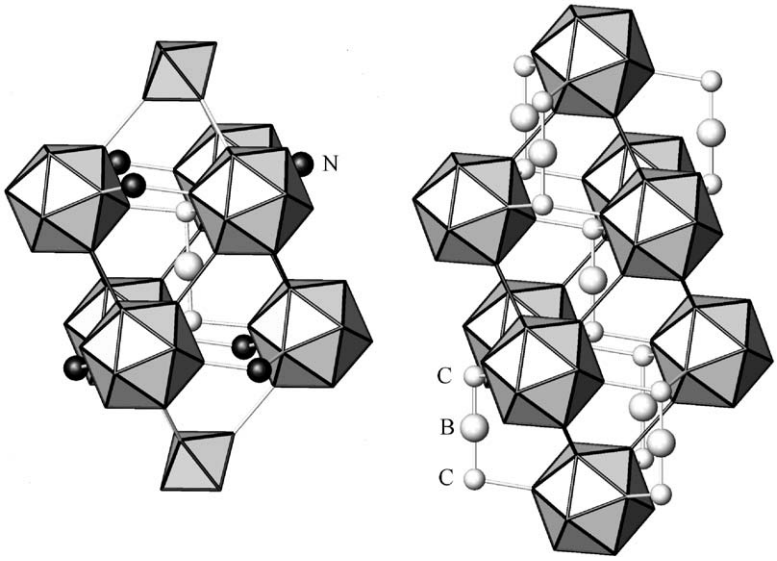

Fig. 2. (a) Coordination environment of the linear [CBC] chain in $Sc_{1-x}B_{15.5}CN$. (b) Coordination environment of the linear [CBC] chain in "B_4C".

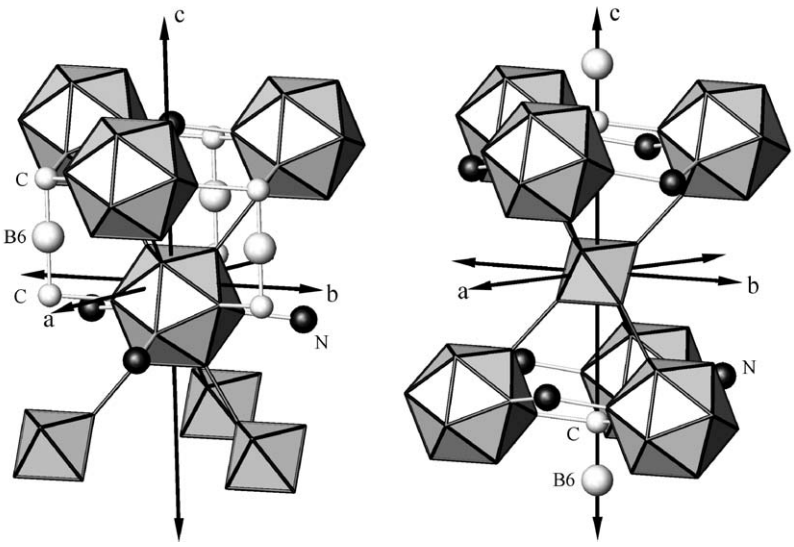

Fig. 3. (a) Environment of the boron $(B_{12})^{ico}$ icosahedra in $Sc_{1-x}B_{15.5}CN$. (b) Environment of the boron $(B_6)^{oct}$ octahedra in $Sc_{1-x}B_{15.5}CN$.

$d_{\text{“BB”}} = 0.1803$ nm and $d_{\text{“BB”}} = 0.1788$ in “B_4C”) (see Table 3), a situation commonly observed in higher borides.

In “B_4C” the interconnection of $(B_{12})^{ico}$ gives rise to planar B_4C_2 six membered rings similar to the planar hexagons observed in graphite. In “B_4C” the [CBC] chain is perpendicular to those rings (see Fig. 2b).

In $Sc_{1-x}B_{15.5}CN$ the situation is insofar slightly different since not only C acts as a bridge (via the [CBC] chains along the c-axis) but also nitrogen forms very tight (see Table 3) $(B_{12})^{ico}$–N bonds. It bridges three icosahedra with a deviation of the bond direction from the normal to the icosahedra by only 0.45°. The sheets of $(B_{12})^{ico}$ clusters are now interconnected in an unique way. Two icosahedra, one C and one N atom participate in hexagonal planes thus composed of 2 CB4, 2 B2B4 and 2 B2N bonds forming the edges of the hexagons (mean $d_{edge} = 0.1639$ nm) with hexagonal angles $116.6° \leqslant \alpha \leqslant 122.8°$ (see Fig. 4). These hexagons form a puckered array of rings (110.34° to the [CBC] chain) which enables a connection of the icosahedra in the a–b plane where there exist no direct inter-icosahedral contacts!

The undistorted octahedra are composed of 6 B5 atoms ($d_{B5B5} = 0.1762$ nm) and are centered at $(0, 0, \frac{1}{2})$. Via 6 B5–B3 inter-cluster bonds the $(B_6)^{oct}$ are connected with the $(B_{12})^{ico}$ (see Fig. 3b).

Nitrogen is not solely bonded to three $(B_{12})^{ico}$ but also to Sc. Since the interstitials of the slab formed by boron iocosahedra are already occupied, Sc resides in rather spacious voids present in the array of boron octahedra (see Fig. 5). While the metal atoms seem to be rather loosely bonded to the octahedral and icosahedral atoms (see Table 3) there exist a strong anchoring connection with the N atom of $d_{ScN} = 0.2133(4)$ nm. In the cubic face centered ScN (NaCl-type of structure) we find

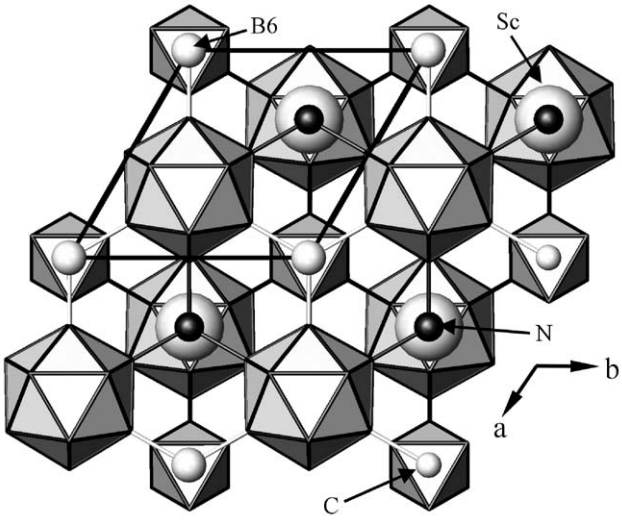

Fig. 4. The structure of $Sc_{1-x}B_{15.5}CN$ projected along the c-axis.

$d_{ScN} = 0.2254$ nm [14] for an octahedral coordination of Sc by N. This fairly anisotropic bonding scheme is also reflected in the thermal parameters of Sc (see Table 2). A similar role of nitrogen is also observed in rhombohedral $MgNB_9$ [15] which crystal structure is closely related to that of $Sc_{1-x}B_{15.5}CN$ and $YB_{22}C_2N$ [2]. There alternating layers of boron icosahedra linked by nitrogen atoms ($d_{BN} = 0.1524$ nm) and boron octahedra form a framework with Mg atoms situated within the $(B_6)^{oct}$ sheets and bonded to nitrogen ($d_{MgN} = 0.2086$ nm) [15].

3.3. Distribution of the light interstitial atoms

The allocation of the different light atomic species to the individual interstitial sites were made based on

structural chemical considerations and the analysis of the electron densities of these sites. Carbon was assigned to position 2c based on the similarity (atomic distances and coordination environment) of the so formed [CBC] unit as observed in "B_4C" [11,12]. No attempts were made to refine similar to "B_4C" [12] boron icosahedra with random substitution of carbon atoms onto polar boron sites. Already in the very initial state of this investigation motivated from difference Fourier calculations the 2*d* ($\frac{1}{3}, \frac{2}{3}, \sim\frac{1}{4}$) site was found to be occupied by an atomic species richer in electrons than boron and carbon therefore most likely by nitrogen. The chemical identity was then confirmed by EPMA and unambiguously revealed by the chemical analysis of isostructural bulk $ErB_{17}C_{1.3}N_{0.6}$.

Comparison of the compositions deduced from the refinement of the crystal structure of $Sc_{1-x}B_{15.5}CN$ with results of EPMA analysis of two independent Sc containing crystal growth batches from different metal fluxes as well as the wet chemical analysis of bulk $ErB_{17}C_{1.3}N_{0.6}$ give rather consistent compositions with an average metal atom to "light" atoms ratio of $\approx$1:19. Since the octahedral and icosahedral boron clusters are very stable structure forming aggregates there is little doubt of vacancies in these arrangements. Therefore disorder and stoichiometric variability most likely come from occupational degree of freedom of the interstitial sites. Already mentioned partial occupancy of the metal sites plays a significant role (if we assume the metal 2*d* site fully occupied the ratio 1:17.5 is the lower limit of the Rare Earth metal to light element proportion in these series of compounds). For the crystal grown from the Sn flux the occupation of the Sc position was refined to 94% and for the one formed in the Si flux an

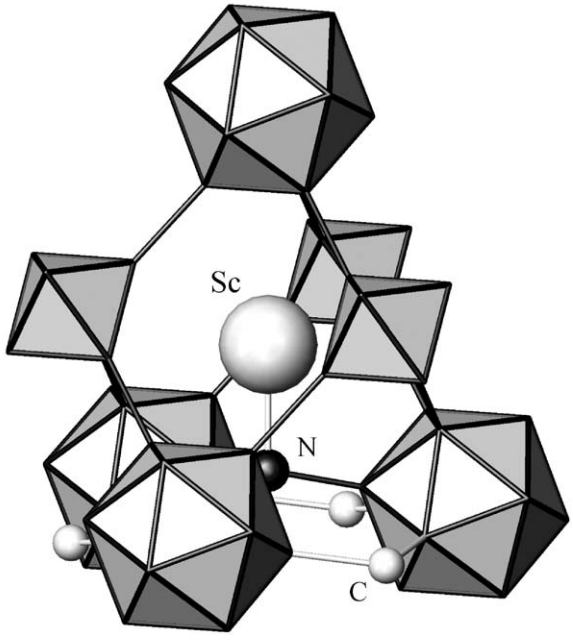

Fig. 5. Coordination environment of the Sc atoms.

Table 3
Selected interatomic distances in $Sc_{1-x}B_{15.5}CN$

Central atom	Ligands	Distances (nm)	Central atom	Ligands	Distances (nm)
Sc	1 N	0.2133(4)	N	3 B1	0.1547(3)
	3 B5	0.2568(3)		1 Sc	0.2130(4)
	3 B3	0.2775(4)			
	6 B5	0.2847(3)			
	3 B1	0.2861(4)	B1	1 N	0.1547(3)
	6 B3	0.3146(5)		2 B4	0.1783(4)
				1 B2	0.1803(4)
C	1 B6	0.1439(4)		2 B3	0.1828(3)
	3 B4	0.1587(3)			
			B3	1 B5	0.1704(4)[a]
B2	1 B2	0.1729(5)[b]		2 B3	0.1788(5)
	1 B1	0.1803(4)		1 B4	0.1794(4)
	2 B4	0.1805(3)		2 B1	0.1828(3)
	2 B2	0.1815(5)			
			B5	1 B3	0.1704(4)[a]
B4	1 C	0.1587(3)		2 B5	0.1763(5)
	2 B1	0.1783(3)		2 B5	0.1762(5)
	1 B3	0.1794(4)			
	2 B2	0.1805(3)	B6	2 C	0.1439(4)

[a] Bonds between $(B_6)^{oct}$ and $(B_{12})^{ico}$.

Table 2
Refined positional parameters and anisotropic displacement parameters for "$Sc_{1-x}B_{15.5}CN$"

Atom	Site	*x*/*a*	*y*/*b*	*z*/*c*	U_{11}	U_{22}	U_{33}	U_{23}	U_{13}	U_{12}	U(nm$^2 \times 10^3$)
Sc	2*d*	1/3	2/3	0.4426(1)	0.0226(5)	0.0226(5)	0.0065(5)	0.0	0.0	0.0113(3)	16.1(4)
B1	6*i*	0.4909(4)	0.5091(2)	0.2177(2)	0.0039(9)	0.0045(1)	0.0049(1)	−0.0005(9)	−0.0003(4)	0.0022(6)	3.8(4)
B2	6*i*	0.5580(1)	0.4420(2)	0.0612(1)	0.005(1)	0.0044(9)	0.003(1)	−0.0004(4)	−0.0007(9)	0.0022(6)	3.5(4)
B3	6*i*	0.7737(2)	0.2263(2)	0.3175(2)	0.0043(9)	0.0043(9)	0.005(1)	0.0006(5)	−0.0006(5)	0.002(1)	4.5(4)
B4	6*i*	0.8383(4)	0.1617(2)	0.1611(2)	0.0042(9)	0.0042(9)	0.004(1)	0.000(4)	0.000(4)	0.002(1)	4.2(4)
B5	6*i*	0.8945(2)	0.1055(2)	0.4331(2)	0.0062(9)	0.003(1)	0.004(1)	−0.0004(9)	−0.0002(5)	0.0016(6)	4.8(4)
B6	1*a*	0	0	0	0.005(1)						
C	2*c*	0	0	0.1338(3)	0.0041(9)						
N	2*d*	1/3	2/3	0.2446(3)	0.0061(8)						

U_{eq}: one-third of the trace of the orthogonalized U_{ij} tensor; thermal factors $T = \exp(-8\pi^2 U[\sin(\theta)/\lambda]^2)$.
Anisotropic thermal factor $T = \exp(-2\pi^2[h^2(a^*)^2U_{11} + k^2(b^*)^2U_{22} + \cdots + 2hka*b*U_{12}])$.
The occupation of Sc was refined to 93(1)%.

Table 4
Lattice constants of REB$_{15.5}$CN (RE= Y, Ho, Er, Tm, Lu)

Compound	Lattice parameters (nm)		Volume (nm^3)	c/a
	a, b	c		
"YB$_{15.5}$CN"	0.55919(6)	1.0873(5)	0.2944(1)	1.944
"HoB$_{15.5}$CN"	0.55883(7)	1.0878(6)	0.2942(2)	1.947
ErB$_{17}$C$_{1.3}$N$_{0.6}$	0.55889(5)	1.0880(6)	0.2943(2)	1.947
"TmB$_{15.5}$CN"	0.5580(1)	1.0850(6)	0.2926(2)	1.944
"LuB$_{15.5}$CN"	0.55771(9)	1.0839(4)	0.2919(1)	1.944

occupation of 91% was found. This is in good agreement with the results deduced from the EPMA analysis. Since all atomic sites in this structure are well localized (proved for the Sc containing compound by a featureless difference Fourier map and the fact that all inter boron cluster bonds are well established) the differences in composition with respect to the carbon and nitrogen content may stem from partial and/or mixed site filling. A similar behavior was observed for rhombohedral YB$_{22}$C$_2$N [2] where different to the REB$_{15.5}$CN series nitrogen can be completely replaced by carbon and therefore seems to be not essential in stabilizing the structure.

3.4. TEM results for $Sc_{1-x}B_{15.5}CN$

HRTEM images taken along the [0001] and [11^{2}0] directions are presented in Fig. 6a and b, respectively. The corresponding electron diffraction patterns (obtained in the selected area diffraction mode) are shown as insets. In Fig. 6a, hexagonal rings of black dots apparent in the high-resolution image can be attributed to Sc atoms seen in the [0001] plane projection. The crystal unit cell contains two hexagonal layers of Sc atoms stacked in the AB configuration, which in projection appears as a honeycomb array (see also Fig. 4). This feature is reflected in the experimental image, and could be easily matched with a simulated image, as shown in the inset. A dark dot situated in the middle of the hexagonal rings is also apparent in both the experimental and the computed image. By comparing with the structure model obtained from the analysis of the X-ray data this image contrast can be assigned to the stacking of boron octahedra and [CBC] chains along the c-axis. In Fig. 6b, the crystal is viewed along its [11^{2}0] zone axis, thus showing the (0001) and the (10^{1}0) repeat distances of the unit cell (1.076 and 0.482 nm, respectively). Again Sc is responsible for the dominant image features, namely the white dots arranged in a zigzag along the [10^{1}0] direction. Although image matching could not be carried out as successfully as in Fig. 6a, additional structural information conveyed by the experimental image is consistent with the proposed model. In particular, the fainter zigzags parallel to the Sc zigzag may be identified as the rows of $(B_{12})^{ico}$ and

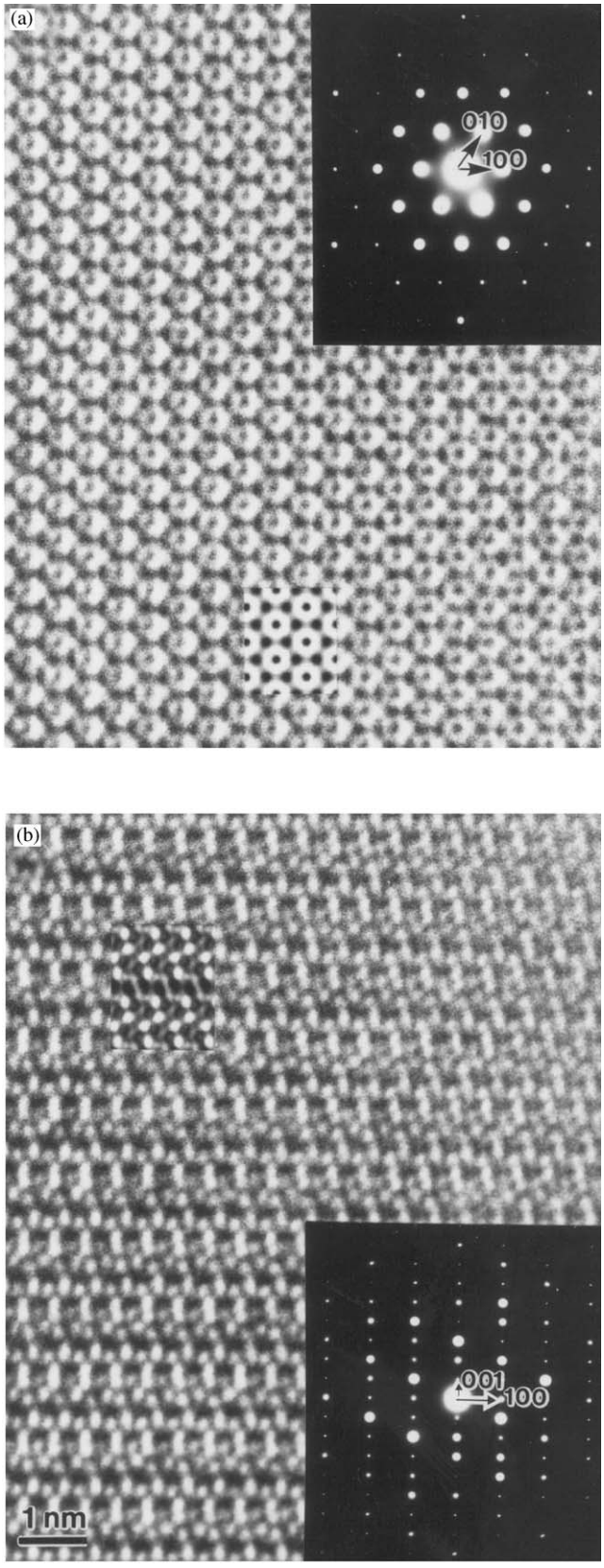

Fig. 6. (a) HRTEM images and electron diffraction patterns taken along the [0001] direction. (b) HRTEM images and electron diffraction patterns taken along the [11^{2}0] direction.

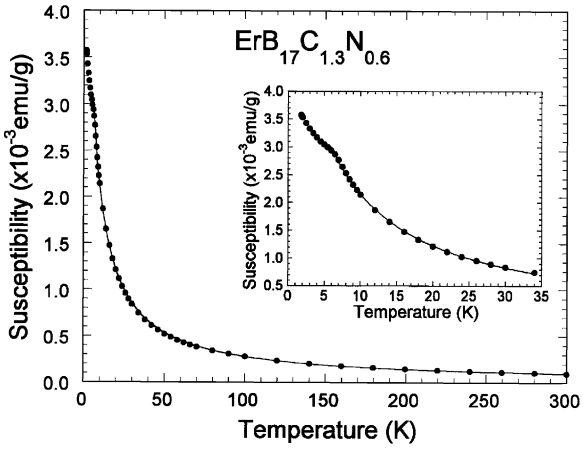

Fig. 7. Magnetic susceptibility of $ErB_{17}C_{1.3}N_{0.5}$ as a function of temperature. (Inset) Behavior at low temperatures.

[CBC] chains. Detailed TEM analysis of $YB_{15.5}CN$ and $YB_{22}C_2N$ [2,3] led to similar conclusions and clearly confirmed the layered stacking of the different boron clusters along the *c*-axis.

3.5. *Magnetic susceptibility of $ErB_{17}C_{1.3}N_{0.6}$*

The static magnetic susceptibility of $ErB_{17}C_{1.3}N_{0.6}$ is given in Fig. 7. Although a slight anomaly is observed below 6 K where there is a downward bend in the susceptibility curve, since the variation is small, we attribute this to an impurity phase and not to an intrinsic magnetic transition of $ErB_{17}C_{1.3}N_{0.6}$. Since small XRD diffraction peaks of ErB_{12} could be observed prior to washing the sample in acid and because the antiferromagnetic transition temperature T_N of ErB_{12} is 6.4 K [16], we conclude the impurity phase to be ErB_{12}. The susceptibility above 6 K can be described well as the sum of a temperature independent term χ_0 and a Curie–Weiss term:

$$\chi = \chi_0 + N\mu_{eff}/3k_B(T-\theta)$$

with $\chi_0 = 9.3 \times 10^{-8}$ emu/g, an effective number of Bohr magnetons μ_{eff} of $9.3\mu_B$/Er atom, and a Curie–Weiss temperature θ of –3.4 K. The small θ is consistent with the fact that no intrinsic magnetic transition is observed in the compound. The magnitude of μ_{eff} agrees fairly well with the value of $9.58\mu_B$/Er atom of free Er^{3+} and thus indicates the Er atoms in $ErB_{17}C_{1.3}N_{0.6}$ are trivalent ions as is the case for other boron-rich erbium compounds.

4. Conclusions

The introduction of nitrogen during the synthesis of rare-earth metal borocarbides gives rise to the formation of a new class of compounds with a rather simple but striking crystal structure. $(B_{12})^{ico}$ icosahedra and $(B_6)^{oct}$ octahedra are bridged by [CBC] chains and nitrogen atoms in an unique way. The structure is closely related to that of "B_4C" and $MgNB_9$. Interstitial sites in this framework can be occupied by *RE*-metals (Y, Ho, Er, Tm and Lu) and Sc. Deviation from full occupancy of the metal site was quantified for the Sc and Er containing compounds. Moreover, based on the arrangement of structural motifs observed in the $REB_{15.5}CN$ compounds a series of homologous phases can be synthesized. Their crystal structure can be derived from that of "B_4C" by systematically replacing icosahedral layers with layers composed of $(B_6)^{oct}$ octahedra and rare-earth metal atoms.

Acknowledgments

This work has been financed by the STA, Japan. We thank Dr. H. Borrmann (MPI-CPfS) for supervising the single-crystal X-ray data collection of a crystal grown from a Sn flux.

References

[1] V.I. Matkovich (Ed.), Boron and Refractory Borides, Springer, Berlin, Heidelberg, New York, 1977.
[2] F.X. Zhang, A. Leithe-Jasper, J. Xu, T. Mori, Y. Matsui, T. Tanaka, S. Okada, J. Solid State Chem. 159 (2001) 174–180.
[3] F.X. Zhang, F.F. Xu, A. Leithe-Jasper, T. Mori, T. Tanaka, J. Xu, A. Sato, Y. Bando, Y. Matsui, Inorg. Chem. 40 (2001) 6948–6951.
[4] F.X. Zhang, F.F. Xu, T. Mori, Q.L. Liu, A. Sato, T. Tanaka, J. Alloys Compd. 329 (2001) 168–172.
[5] A. Leithe-Jasper, L. Bourgeois, Y. Michiue, Y. Shi, T. Tanaka, J. Solid State Chem. 154 (2000) 130–136.
[6] A. Altomare, G. Cascarano, C. Giacovazzo, A. Guagliardi, J. Appl. Cryst. 26 (1993) 343–350.
[7] G.M. Sheldrick, SHELX97: A Programme for the Solution and Refinement of Crystal Structures, Universitaet Goettingen, Goettingen Germany, 1997.
[8] E. Dowty, ATOMS 4-1, Shape Software, Kingsport, TN, USA, 1998.
[9] Y. Shi, A. Leithe-Jasper, T. Tanaka, J. Solid State Chem. 148 (2000) 250–259.
[10] P. Rogl, J. Schuster, Phase Diagrams of Ternary Boron Nitride and Silicon Nitride Systems, ASM International, Materials Park, OH, USA, 1992.
[11] A. Kirfel, A. Gupta, G. Will, Acta Crystallogr. B 35 (1979) 1052–1059.
[12] M. Dutheil, G. Baldinozzi, D. Simeone, A. Leithe-Jasper, Phys. Rev. B, 2003, in print.
[13] H.C. Longuet-Higgins, M.V. de Roberts, Proc. Roy. Soc. London A 230 (1955) 110–119.
[14] R. Niewa, priv. commun., 2002.
[15] W. Jung, M. Fayerman, Proceedings of the 14th International Symposium on Boron, Borides and Related Compounds, St. Petersburg (Russia), June 9–14, 2002, p. 65.
[16] B.T. Matthias, T.H. Geballe, K. Andres, E. Corenzwi, G.W. Hull, J.P. Maita, Science 159 (1968) 530.
[17] A. Leithe-Jasper, T. Tanaka, unpublished research, 1999.
[18] A. Leithe-Jasper, T. Tanaka, Proceedings of the 13th International Symposium on Boron, Borides and Related Compounds, Dinnard (France), September 5–10, 1999, p. O22.